RESIDUAL GAS FLUORESCENCE FOR PROFILE MEASUREMENTS AT THE GSI UNILAC

P. Forck and A. Bank
Gesellschaft für Schwerionenforschung GSI, Darmstadt, Germany
e-mail: p.forck@gsi.de

Abstract

The pulsed heavy ion LINAC at GSI (UNILAC) delivers such a high beam current, that intersecting diagnostics like profile grids can be destroyed within one macro-pulse. As an alternative method we investigate the monitoring of the fluorescence light emitted by the N_2 molecules of the residual gas at blue (molecular ion: 400 to 470 nm) and near UV (neutral molecule 330 to 410 nm). The design parameter of the image intensifier and the IEEE 1394 (Firewire) CCD camera are discussed. Measurements with short (about 1 ms) beam pulses of several 100 μA heavy ions prove the good applicability of the method.

1 RESIDUAL GAS FLUORESCENCE

The profile of an ion beam can directly be determined by monitoring the fluorescence emitted by the residual gas molecules using a sensitive image intensifier coupled to a CCD camera. This method was previously applied e.g. at cw proton LINACs at Los Alamos [1] and the CERN SPS synchrotron [2]. Here a test at the pulsed heavy ion LINAC at GSI [3] is done to monitor the profile within one macro pulse of about 200 μs length, e.g. used to fill the proceeding synchrotron. The short beam delivery times disable the possibility for long integration times normally used to improve the signal-to-noise ratio. The new design uses a digital CCD camera, which fits to the need of distributed beam diagnostic device within a large accelerator facility.

The traditional determination of transverse beam profile by secondary emission grids (SEM-grids) can not be applied at the high current operation with up to 20 mA electrical current for the full macro-pulse length due to the large energy release of the ion beam (maximal 1 MW beam power) in the intersecting material. Not to risk melting, the macro-pulse length has to be shorted. For the full pulse length a non-intersecting residual gas monitor can be used or the fluorescence of the residual gas can be detected. The later has the advantage that no mechanical parts, and therefore no extra apertures are installed in the vacuum pipe, leading to a compact and cost efficient design. In addition, the spatial resolution for a SEM-grid is limited by the wire spacing of about 1 mm. Using the fluorescence method, up to 0.1 mm can be achieved. Another advantage is the compact commercial 'data acquisition system' incorporated in the CCD camera.

At the GSI LINAC the ion's kinetic energy varies from 0.12 MeV/u after the first module up to the final LINAC energy of 15 MeV/u. Depending on the ion species and its charge state, this is close to the maximum of the electronic stopping power. The residual gas at the LINAC has a typical pressure of 10^{-7} mbar containing mainly Nitrogen.

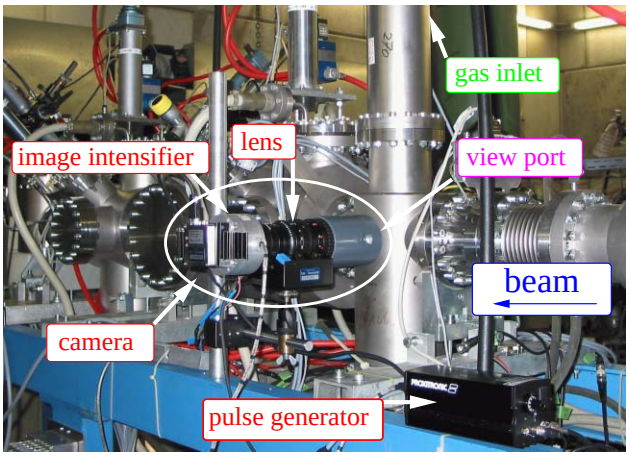

Figure 1: The installation of the intensified camera at the target location.

N_2 has a large cross section for the excitation in the neutral and ionized N_2^+ molecular states, as measured in [4] by 200 keV proton collisions. Due to the non-resonant excitation process, a scaling proportional to the electronic stopping power of the beam ions is expected. Via optical transitions two bands are emitting in the blue and near UV range, namely the ionized N_2^+ at a band $B^2\Sigma_u^+ \rightarrow X^2\Sigma_g^+$ with prominent peaks at 391 nm, 428 nm and 470 nm. The upper state $B^2\Sigma_u^+$ can be accessed by a single step excitation. At slightly shorter wavelength prominent transitions within the neutral N_2 $C^3\Pi_u \rightarrow B^3\Pi_g$ band is observed with lines between 358 nm and 408 nm. Only by a two step process the upper level is populated due to the necessary spin flip with respect to the neutral $X^1\Sigma_g^+$ ground state. The lifetime of both levels had been determined [5] to be about 60 ns for the ionic and 40 ns for the neutral state. Measurements at GeV proton and ion beams (CERN SPS) [2] confirmed the results determined at much lower energies.

2 IMAGE INTENSIFIED CCD CAMERA

Tests are done at a target location, where the beam is viewed through a Suprasil (wavelength transmission between 200 nm and 2 μm) window mounted on a Ø 35 mm flange, resulting in a ∼5 cm observation length in beam direction. To suppress reflections, the tube is blackened by vacuum suitable graphite lacquer (graphite grains solved in isopropanol). The emitted fluorescence is detected by an image intensified camera with a total detection efficiency of ∼10 % of the photons arriving at the photo-cathode. The main components of the system are shown in Fig. 1 and de-

scribed in the following:

Zoom lens: A remote controlled C-mount zoom lens (Fujinon D14×7.5A-R11/12) with $7.5 - 105$ mm focal length and a macro setting was installed having it's image plane 39 cm apart from the beam center. A short distance is preferred to capture more photons due to a large solid angle. A small focal length results in a larger depth of focus, i.e. with the same relative iris setting a large depth can be imaged.

Image intensifier: The light is converted to electrons by a photo-cathode made of S20 UV-enhanced [6], having a quantum-efficiency of $25 - 30\%$ at the interesting wavelength interval and a low dark current (∼500 electrons/s·cm^2). The voltage between the photo-cathode and the following Multi Channel Plate (MCP) can be switched from a blocking mode for the photo-electrons to a transfer mode within 100 ns enabling an observation only during the beam delivery. This reduces drastically the background given by dark counts i.e. spontaneous emission of photons from the photo-cathode or the MCP. In addition, a possible beam width variation within the macro pulse is observable using this switching. A two-fold MCP Ø 25 mm amplifies the photo-electrons with a gain of $\sim 10^6$. On the following P46 fast phosphor screen a spot from each of the single photo-electrons is visible. Due to the phosphor decay time of ∼300 ns (90% to 10 %) fast changes of the beam parameters can be resolved. The spatial resolution of ∼0.1 mm on the MCP surface is sufficient for our application.

Taper coupling: For the light transmission from the Ø 25 mm phosphor to the 1/2"standard Sony CCD chip (6.4×4.8 mm^2) we used a minifying taper coupling made of bundled glass fibers and a minification of 8/25 (ratio of CCD and MCP diameter). About 7 % of the light emitted in the half hemisphere is guided to the CCD. As compared to relay optics made by a second standard lens combination a factor of ∼5 higher light transmission is achieved. The disadvantage of this choice is, that the CCD chip cannot be exchanged easily in case of a ruination by the radiation level produced by the beam.

CCD camera: The modern type 8 bit CCD camera Basler A302fs were chosen with 782×582 pixels. The accumulated charges of the pixels are directly digital-converted at the camera head and transfered using Firewire IEEE 1394 protocol. Compared to an analog video link, no degradation of the image quality due to long cable occurs. The modern Firewire serial bus standard [7] enables a data rate up to 400 Mb/s, corresponding to more than 100 frames per second. The possible variable bus architecture with up to 63 nodes is well suited for the distributed diagnostic installations in the various beam lines. The maximum cable length for electrical transmission is 5 m. Therefore fiber optic cables driven by opto-couplers (NEC or Newmex Technology) are used for the data transfer to the control room.

Data analysis: After translation from the optical fiber transmission to electrical signals, a cheap standard PCI interface is installed in a WINDOWS PC. The analysis software is written in LabView. It uses the Firewire driver for the commercial package IMAQ to acquire the images and IMAQ Vision for the image processing.

First measurements were performed with a commercial intensified video camera (Proxitronic NANOCAM HF4), equipped with a S20/Quartz photo-cathode and a double MCP. The digitalization was done with a frame grabber.

3 TEST MEASUREMENTS

Medium and high current Ar^{10+} beam (0.5 to 5 mA electrical current) is used for the first tests with energies of 4.7 MeV/u, 5.8 MeV/u and 11.4 MeV/u. In Fig. 2 the image of a single macro pulse with a 5.8 MeV/u Ar^{10+} beam with an electrical current of 700 μA and a pulse length of 200 μs is displayed. This corresponds to $\sim 10^{11}$ particles per macro-pulse passing the view-port for the camera. With the help of a regulated gas valve, the pressure can be raised locally up to 10^{-4} mbar. Due to high amplification of the double MCP 'single photon events' are visible, i.e. each of the spots seen on the 2 dimensional image correspond to one photo-electron. Projecting the collected light along the beam axis results in the vertical profile. The relatively broad beam setting of 13.6 mm FWHM is clearly seen resulting from the sufficient statistics of the arriving fluorescence photons. The resolution of 280 μm/pixel is sufficient for these parameters. For images of less signal strength the data can be binned. Due to the statistical nature of the signal generation, the quality can also be enhanced by summing up several images.

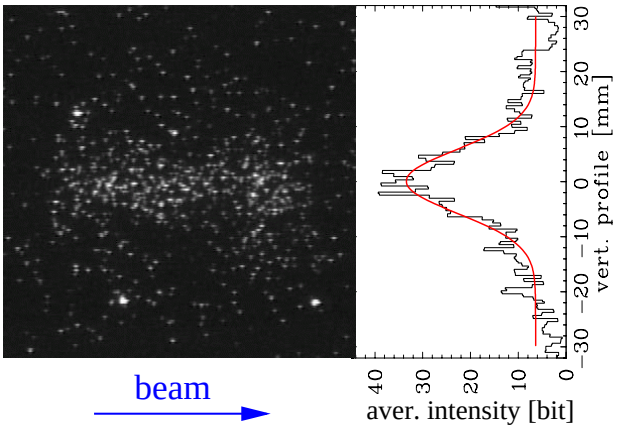

Figure 2: Image of a 200 μs Ar^{10+} beam of $I_{beam} = 700$ μA recorded at the GSI LINAC with a vacuum pressure of 10^{-5} mbar. The two dimensional image from the intensifier (left) and the projection for the vertical profile (right) is displayed.

The measurements show a low background, even without using any optical filters. The uniformly distributed dots outside of the beam path seen in Fig. 2 are caused by γ- or x-rays hitting the photo-cathode generated by nuclear- or atomic inner-shell excitations probably at the beam dump located 2 m apart. Their contribution is independent of the

optical setting, even by a completely closed iris. This unfocused background seems to increase with energy, for 11.4 MeV/u we had a factor ∼4 more than for 4.7 MeV/u. But after projection, its contribution is much weaker than the signal.

Within one order of magnitude, the pressure had been varied and the integrated signal strength shows a linear behavior, confirming previous measurements [2]. The dominant contribution of single step excitations, like the mentioned the N_2^+ $B^2\Sigma_u^+ \rightarrow X^2\Sigma_g^+$ transitions is verified by that.

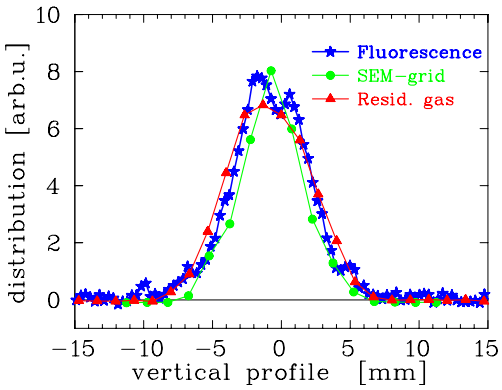

Figure 3: Comparison of the fluorescence profile measurement with a 16 wire SEM-grid located 20 cm down stream for a 4.7 MeV/u Ar^{+10} beam of ∼2.5 mA electrical current. The third curve is the determination by a residual gas monitor. The curves are normalized to the same integral.

In Fig. 3 the measured profile is compared to a SEM-grid located 20 cm downstream. The correspondence is quite well. Even though the fluorescence signal is ∼10 % broader, which might be a result of a slightly wrong setting of the optics (see below). In addition the calibration (pixel-to-mm) has an uncertainty level of about 5 %. But there is no pronounced artificial broadening observed in our environment, neither due to a significant movement of the N_2^+ in the beam space charge potential prior to the light emission nor the excitation of long lived fluorescence states of the N_2, other residual gas components or beam ions. In Fig. 3 the signal from a residual gas monitor is shown in addition, which is about ∼20 % broader compared to the SEM-grid. This is due to the curvature of the N_2^+ trajectories in the space charge potential: the drift time for the N_2^+ from the beam center to the electrode of the residual gas monitor is ∼300 ns, i.e. longer than the fluorescence decay constant of 60 ns.

A crucial point for the operation of the fluorescence monitor is a proper alignment of the optics. In particular the focal distance has to be chosen to coincide with the center of the beam to yield a sufficient large depth of focus. As shown in Fig. 4 a sharp image, and therefore a proper width reading, is only created by a partial closed iris. The total light intensity is reduced, in the shown case by one order of magnitude. In future we will improve the alignment by installing an array of LEDs opposite to the camera on a feed-trough, yielding a precise focal distance setting and

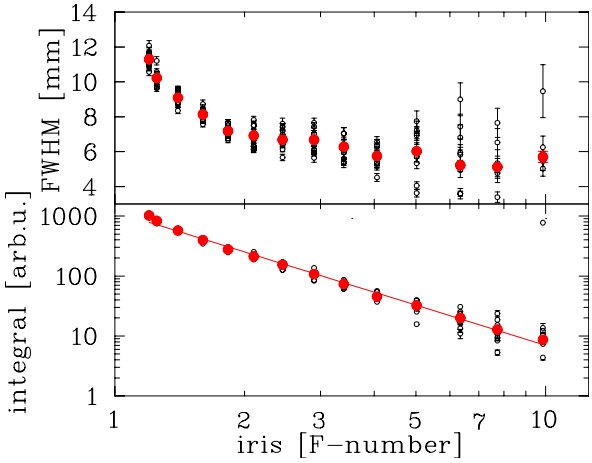

Figure 4: The profile width and the total intensity as a function of the iris setting for the same parameters as in Fig.3. The individual images are shown as thin dots and the average of 10 macro-pulse as thick dots.

an on-line calibration for the pixel-to-mm factor.

4 CONCLUSION

The described non-intersecting method for profile measurements can be applied for ion beams of high current at a pulsed LINAC. For a signal enhancement at lower currents, a moderate pressure bump can to be applied easily. For beams at the first section of the GSI-LINAC, before the stripper, the particle current is an order of magnitude higher as well as the energy deposition, therefore this pressure bump is not needed. A direct image of the beam with low background is generated without any installations inside the vacuum pipe leading to a cost efficient design. The alignment of the optics is a crucial point and has to be controlled on-line. The resolution can be higher compared to a SEM-grid, 0.1 mm is reachable by large magnification. The method offers also more advanced detection schemes, like to observation of a possible beam movement during the macro-pulse. A short exposure time down to 10 μs can be applied by the switching of the photo cathode voltage allowing a signal generation only during this short period.

Acknowledgment: We like to thank A. Peters and A. Weiss for valuable discussions and many practical support.

5 REFERENCES

[1] D.P. Sandoval et al., 5^{th} *Beam Instrum. Workshop, Santa Fe, AIP Conf. Proc. 319*, p. 273 (1993).

[2] G. Burtin et al., *Proc.* 6^{th} *Euro. Part. Acc. Conf. EPAC, Vienna*, p. 256 (2000).

[3] W. Barth, *Proc.* 20^{th} *LINAC Conf,, Monterey*,p.1033 (2000).

[4] R.H. Hughes et al., *Phys. Rev.* **123**, 2084 (1961).

[5] L.W. Dotchin et al., *J. Chem. Phys.* **59**, 3960 (1973).

[6] www.proxitronic.de.

[7] D. Anderson, *FireWire system architectur: 1394a*, www.mindshare.com, Addison-Wesley (1999).